Nonlinear-resonance Analysis of Halo-formation excited by Beam-core Breathing

Yoshito SHIMOSAKI and Ken TAKAYAMA *
Department of Energy Science and Engineering, Kyushu University
6-4-1, Hakozaki, Fukuoka-shi, Fukuoka, 812-8581, Japan
* Accelerator Laboratory, High Energy Accelerator Research Organization (KEK)
1-1, Oho, Tsukuba-shi, Ibaraki, 305-0801, Japan

Abstract

Emittance growth and halo formation for a mismatched beam of a 1D Gaussian distribution in a uniform focusing channel are examined by means of macro-particle simulation. The results are analyzed by the isolated nonlinear resonance theory. The second-harmonic resonance driven by beam core oscillation is numerically and analytically shown to take a key role in forming halo. Analytic estimation of the halo-location is explored and the halo-location is proved to correspond to the outer edge of the resonance islands. Nonlinear fields in an actual particle distribution are shown to significantly affect on the halo's location and size.

1 Introduction

One of major issues in high power accelerators is activation of accelerator components due to beam loss. Beam loss has to be reduced to the order to allow hands-on-maintenance. In order to produce an acceptable design, it is important to understand the mechanisms of emittance growth and halo formation resulting in beam loss.

Most of recent attention has been focused on driver linacs. Totally self-consistent particle in cell simulation (PIC) codes have been developed, which have demonstrated a wide variety of aspects in halo formation for realistic beam distributions [1]. Meanwhile, the analysis and understanding of space charge effects for particle beams in linacs has been greatly facilitated by use of particle core models (PCM). Resonant (parametric) interaction between the breathing core and the individual particle oscillating about and through the beam core as the driving mechanism of halo formation has been explored on this model by many research groups [2,3]. Certainly, PCMs are useful for qualitative understanding of the halo formation mechanism and the explored mechanisms are suggestive for a more realistic distribution. However, there is no confidence to be capable of quantitatively estimating the size of halo and its parameter dependence.

In the contrast to the case in linacs, understanding of the halo formation mechanisms in circular rings seems to be quite difficult even by the PIC codes for a realistic distribution, because repeated betatron oscillations through a huge number of lattice elements takes a key role in the resonant interaction and the numerical calculation over a sufficient number of turns should take unrealistic CPU times and memory. We have a strategy to develop a useful analytic model capable of predicting position of halo in a real space as a function of beam and machine parameters, for a realistic beam distribution. As the first step of this strategy, halo formation in a 1D Gaussian distribution in a uniform focussing channel has been numerically examined and a second-harmonic nonlinear resonance excited by the rms beam core oscillation has been identified to be a driving mechanism of halo formation. This view has been confirmed by an analytic approach based on the isolated nonlinear resonance theory. The simulation and theory have shown that highly nonlinear components in the real distribution strongly affect on the halo location. The current analytic approach is believed to be a germinal model in the future theory dealing with a 2D realistic distribution in the FODO lattice.

2 Multi-particle Simulation

First of all, a 1-D simulation method is described which has been used to understand detail and dynamic process in involved physical phenomena. Through the simulation, a beam distribution is assumed to be of infinite and uniform in the horizontal and longitudinal planes and finite and non-uniform in the vertical plane. In addition, the beam propagates through free space. Space-charge fields affect on the betatron motion of beams in vertical direction.

The vertical electric field originated from beam space-charge in the rest frame is written in the form of $E_y(y) = e\left[\int_{-\infty}^{y} n(y')dy' - \int_{y}^{\infty} n(y')dy'\right]/\varepsilon_0$, where $n(y)$ is a particle density function in the rest frame. In general, $E_y(y)$ is nonlinear with respect to y. Perturbing effects of nonlinear fields are included as delta-function like kicks

$$\begin{pmatrix} y_{s+\Delta s} \\ y'_{s+\Delta s} \end{pmatrix} = \boldsymbol{M}\begin{pmatrix} y_s \\ y'_s \end{pmatrix} + \begin{pmatrix} 0 \\ \dfrac{eE_y(y_{s+\Delta s})}{\gamma m v^2}\Delta s \end{pmatrix}, \tag{1}$$

where $\boldsymbol{M}$ is the transfer matrix of linear focusing system, m is rest mass of particle, γ is a relativistic mass factor, v is the velocity of the design particle and Δs is the longitudinal step. Numerical integration of $n(y)$ with linear interpolation gives E_y, which is assumed to be constant through Δs, at the exit of step.

We plan to apply the current study for the 12GeV proton synchrotron (KEK-PS). Most of calculating parameters are very similar to that of the KEK-PS where C = 340m is the circumference, ν_y = 6.23 is the bare tune and the injection energy is 500MeV. In order to manifest a key roll of space charge effects in halo formation, an extremely high current has been studied here. In simulations, 10^5 macro particles have been tracked over more than 100 turns. For choosing

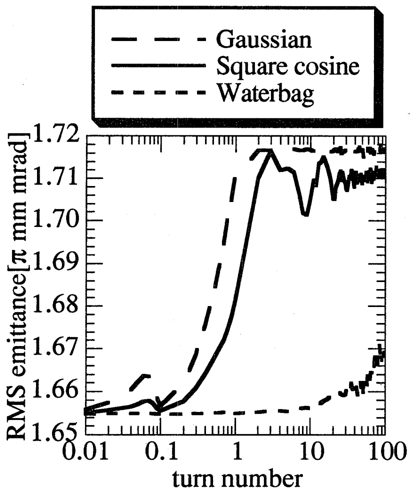

Fig. 1 RMS emittance growth of the mismatched beams

Δs, saturation in the simulation results has been monitored as a function of Δs and $\Delta s = 5\,\text{cm}$ has been applied.

For justification in the simulation scheme, an exact equilibrium Gaussian distribution analytically derived by Vlasov's equation and, for comparison, an other exact equilibrium Gaussian distribution function without space-charge effects were put into calculation as an initial condition of the simulation. The former RMS emittance does not change much with growth less than 0.3% and the later quickly grows to saturate with a big growth of about 4%. Thus the simulation scheme has been conformed to give a reasonable results.

3 Steady states for mismatched Gaussian, waterbag and square cosine distribution

Now we call a beam, which has the exact equilibrium distribution function with space-charge effects, as "a matched beam" and other beams as "mismatched beams". The simulations were carried out for three cases of mismatched beams with Gaussian, waterbag and square cosine distribution. The square cosine distribution is defined as $f(y,y') = f_0 \cos^2\left(\pi\sqrt{y^2+y'^2}\,/\,2R(y,y')\right)$, where $R(y,y')$ is the distance from the origin to the outer edge through (y, y'). It is noted that its profile is continuous at the beam boundary as that of a Gaussian distribution and the beam edge is finite as that of a waterbag distribution. All initial distribution functions have the same total current and the same RMS emittance as the matched beam.

RMS emittance growth of the mismatched beams is shown in Fig. 1. Gaussian and square cosine distributions quickly arrive at steady states after less than a few tens of turns (≤ 3 for Gaussian and ≤ 30 for square cosine). Meanwhile, the RMS emittance of the waterbag beam still grows over 1200 turns. The beam density with the square cosine distribution at first approaches to the Gaussian distribution at the steady state. On the other hand, the beam with the waterbag distribution tends to become flat because

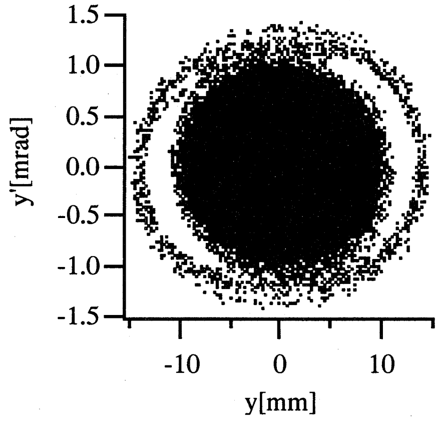

Fig. 2 The phase space projection at 100th turn

of redistributing towards the beam edge.

The phase space projection of the beam with the square cosine distribution after 100$^{\text{th}}$ turn suggests that particles escaping from the core are responsible for the growth of RMS emittance. In addition, it is remarkable that there are two vacant regions as seen in Fig. 2. This particle redistribution seems to originate from nonlinear resonances. Test particles of 10 were put in one vacant region with some amplitude and trucked after another 100 turns. All oscillation frequency spectra of the test particles obtained by FFT indicate the sharp peaks at $\nu_\beta = 5.23$, where ν_β is the net betatron tune depressed by space-charge forces. Since the oscillation frequency should depend on the amplitude because of the nonlinear space-charge fields, this means the motions of test particles are dominated by nonlinear resonance.

Since there are no external nonlinear fields in the uniform focusing channel, the sources driving nonlinear resonances are identified to be the self space-charge fields. The simulation results also show the notable oscillation of the RMS beam size, which is simply induced by mismatching. Parametric resonance between a single particle motion and the beam core oscillation can be exited when the depressed betatron tune ν_β and the tune of core oscillation ν_c satisfy $\nu_\beta / \nu_c = i / j$, where i and j are integer. The lowest dominating resonance is obviously a second-harmonic resonance, which is capable of creating two resonance islands. Certainly, the FFT of the core oscillation exhibits a single sharp peak at $\nu_c = 10.45$. The results strongly suggest the major source of the second-harmonic resonance is the rms beam core oscillation.

4 Nonlinear resonance excited by beam core breathing

In order to confirm a speculation suggested by the simulation results that the rms beam core oscillation is capable of driving the second-harmonic resonance, we have developed an analytic approach using the isolated resonance Hamiltonian. Here, the beam distribution is assumed to be the Gaussian distribution with the rms beam size oscillating at a single frequency, $\sigma(s)=\sigma_0(1+\delta\cos\omega_c s)$, where σ_0 is the averaged rms beam size, δ is the maximum deviation from σ_0 and $\omega_c=2\pi\nu_c/C$ is the frequency of the beam core oscillation. Then the Gaussian distribution in the rest frame is given by $n(y,s)=N_0\exp(-y^2/2\sigma(s)^2)/\sqrt{2\pi}\sigma(s)$, where N_0 is the total number of particles per unit length in the rest frame. The electric field of this is written in the form of the Taylor expansion,

$$E_y(y,s)=\frac{eN_0}{\varepsilon_0\sqrt{2\pi}}\sum_{n=0}^{\infty}\frac{(-1)^n}{n!(2n+1)2^n}\frac{y^{2n+1}}{\sigma(s)^{2n+1}}. \quad (2)$$

Introducing the action-angle variables (ϕ,J), the single particle Hamiltonian is expressed as

$$H=\omega_\beta J-A\sum_{n=0}^{\infty}\frac{(-1)^n}{n!(2n+2)(2n+1)}\left(\frac{J}{\sigma_0{}^2\omega_\beta}\right)^{n+1}F_n(\phi,s), \quad (3)$$

where $A=2\sigma_0 e^2N_0/\gamma^2\varepsilon_0 mv^2\sqrt{2\pi}$, $\omega_\beta=2\pi\nu_y/C$ is the bare betatron frequency and in a case of δ<<1 of our interest, $F_n(\phi,s)=\{1-(2n+1)\delta\cos\omega_c s\}\cos^{2n+2}\phi$.

The rapidly oscillating terms except the slowly oscillation terms disappear after averaging Eq. (3) over many turns [4]. The later excites the second-harmonic resonance. The averaged Hamiltonian, called the isolated resonance Hamiltonian, H_{iso} is written by

$$H_{iso}=\left(\omega_\beta-\frac{\omega_c}{2}\right)J-A\sum_{n=0}^{\infty}a(n)J^{n+1}\left[\frac{1}{n+1}-\frac{2n+1}{n+2}\delta\cos 2\psi\right], \quad (4)$$

where $a(n)=-(2n)!/\{(n!)^3(n+1)(-4\sigma_0{}^2\omega_\beta)^{n+1}\}$ and $\psi=\phi-\omega_s s/2$.

The position and size of the resonance islands are well known to be a good measure to represent the relative strength of perturbing terms. The stable fixed point at $\psi=\pi/2$ and $3\pi/2$ radian and the unstable fixed point at $\psi=0$ and π radian are analytically evaluated by setting the canonical equations to be zero. Maximum and minimum values of the action variable along the trajectory through the unstable fixed point are defined as $J_{\max}$ and $J_{\min}$, respectively. The size of the resonance island (resonance width) is written by $J_{\max}-J_{\min}$ on the action axis.

In order to obtain a necessary and sufficient limit $n_{\max}$ in the above summation, $J_{\max}$ and $J_{\min}$ have been calculated as functions of $n_{\max}$. From the results, $n_{\max}$ must be more than 11. Lower $n_{\max}$ brings the wrong results. Here, $n_{\max}=15$ has been applied.

Calculations of $J_{\max}$ and $J_{\min}$ are performed using Eq. (3), provided the values of σ_0, ω_0 and δ at the steady-state achieved after the transient process, which depend on the initial state. Five sets of the parameters are obtained, assuming the initial states with the same distribution $\sigma_{\rm rms}$ but different beam density N_0. The $J_{\max}$ and $J_{\min}$ are calculated employing each set of above parameters. The calculated locations of resonance islands are in good agreement with the simulation results as shown in Fig. 3. We conclude that the second-harmonic resonance is driven by the beam core oscillation for the nearly Gaussian distribution. In addition, Fig. 3 clearly indicates that the outer edge of the resonance islands can be regarded as the location of halo.

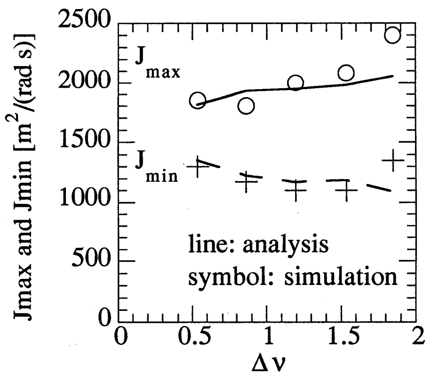

Fig. 3 $J_{\max}$ and $J_{\min}$ vs. $\Delta\nu$

5 Conclusion

Parametric interactions between a core oscillation and a highly nonlinear motion of individual particle drive the second-harmonic resonance for a 1D Gaussian distribution. This supports the speculation of Gluckstern for a realistic beam distribution. The second-harmonic resonance is a source of emittance growth and results in beam halo which is created as an outer edge of the resonance islands. The location of halo is analytically tractable using the canonical equations derived from the isolated resonance Hamiltonian. Nonlinearity in the particle motion is crucial to determine the location of halo; the second-harmonic terms down-fed from higher-order nonlinear terms are included in order to accurately estimate the halo location. The estimation of the halo-location would provide a reasonable choice of physical aperture or halo collimator in proposed high intensity proton accelerators.

Applications of the developed analytic tool for a more realistic 2D distribution in a periodic focusing seem to be straightforward.

References

[1] H. Okamoto and M. Ikegami, Phys. Rev. E **55**, 4694(1997)

[2] J. A. Holmes, J. D. Galambos, D. K. Olsen and S. Y. Lee, *Proc. 1999 Pat. Accel. Conf.*, p279

[3] R. L. Gluckstern, W. Cheng, S. S. Kurennoy and H. Ye, Phys. Rev. E **54**, 6788(1996)

[4] *Physics of Particle Accelerators*, edited by M. Month and M. Dienes, AIP Conf. Proc. No. 153